

Modelling of Channel, Path loss and Capacity analysis for 5G Millimeter-Wave Wireless Systems

Vikram Singh(16104100), Koushik Balasubramanyam(16104044)

Abstract—With limited amount of research done on mm-wave mobile communication an extensive study is done to gain insights on path loss ,building penetration and reflection characteristics for future mm-wave systems.Due to evergrowing exponential demand of voice,data and multimedia services the limited capacity spectrum ranging from 700MHZ to 2.6GHZ may not be sufficient in the coming fututre,hence there is need of more bandwidth which can be extracted from the mm-wave bands.Today the global spectrum bandwidth allocation is 80MHZ with each major provider haveing 200MHZ of spectrum across all frequencies.This study includes the improve- ments of 5G over 4G and how /why it can/should be implemented effectively while analysing its drawbacks.In last we will focus on the mathematical modeling of path loss and estimation of channel using requisite number of FIR taps by calculating spatial autocorrelation function.

I. INTRODUCTION

As the demand for capacity is increasing the wireless carriers should be capable of supporting a thousand fold increase in total mobile traffic by 2020.Improving the existing LTE network ti meet the IMT advanced requirement that feature theoretical speeds that exceed 1Gbps.LTEAdvanced supports heterogeneous networks with co-existing large macro, micro, and pico cells, and Wi-Fi access points.Cost is also a major factor whcih will be realised using repeaters and relays.The main differences compared to 4G are

- 1) The use of much greater spectrum allocations at untapped mm-wave frequency bands.
- 2) Highly directional beamforming antennas at both the mobile device and base station,
- 3) Longer battery life of cellular devices.
- 4) Lower outage probability.
- 5) Very high bit rates in most portions of the coverage area.
- 6) Lower infrastructure costs.
- 7) Higher aggregate capacity for many simultaneous users in both licensed and unlicensed spectrum .

The backbone networks of 5G will move from copper and fiber to mm-wave wireless connections, allowing rapid deployment and mesh-like connectivity with cooperation between base stations.It has been observed that the lifespan of every new generation is approximately a decade due to continous evolution of communication technology. The CMOS technology can operate well in the mm-wave bands and this along with high gain steerable antennas at both Mobile and base station show that mm-wave has ability to survive for long.These steerable antennas and mm-wave spectrum could simultaneously support mobile communication and backhaul along with con-

vergence of WiFi and cellular systems.Presently 4G systems has maximum bandwidth of 20 MHz .By increasing this RF channel bandwidth one can get high speed and low latency.Mm-waves due to it low wavelength (high frequency) can exploit polarization along with Massive MIMO and adaptive beamforming. Uplink current disjoint spectrum allocation mm-waves frequencies will have allocation that are much closer together so as to make the propagation characteristics of different mm-wave bands comparable and homogeneous.The currently available bands are 28GHz and 38GHz with allocations o over 1GHz of bandwidth. The major drawback of mm-waves were its proneness to rain ,however nowadays (atleast in urban scenario) the base station are placed very near to each other in-orders of 200-400m.In such small cell sizes atmospheric absorption does not create too much path loss to disrupt proper communication

Massive MIMO base stations and small-cell access points are two approaches for future cellular systems. Massive MIMO base stations allocate antenna arrays at existing macro base stations, which can accurately concentrate transmitted energy to the mobile users . Small cells offload traffic from base stations by overlaying a layer of small cell access points, which actually decreases the average distance between transmitters and users, resulting in lower propagation losses and higher data rates and energy efficiency.The very low wavelengths allow hundreds of antenna elements to be placed in an array on a relatively small physical platform at the base station, or access point, and the natural evolution to small cells ensures that mm-wave frequencies will overcome any attenuation due to rain. In order to create a statistical spatial channel model (SSCM) for mm-wave multipath channels, extensive measurements must be made in all operating conditions. The penetration measurement show that tinted glass and brick pillars (typical exterior surfaces of urban buildings) have high penetration losses which indicates that building penetration of mm-waves will be difficult for outdoor transmitters, thus providing high isolation between outdoor and indoor networks.But common indoor materials such as clear non-tinted glass and drywall have comparatively less penetration losses. Propagation data is grouped into three subsections: signal acquired , signal detected, and no signal detected.Signal acquired is defined as a location where the SNR is sufficiently high for accurate acquisition, i.e. penetration loss relative to free space test is less than 64 dB. Signal detected is a location where the SNR is detected noise but not strong enough to be acquired. No signal detected denotes an outage, where the penetration loss is at least 74 dB greater than the free space test.It is seen that

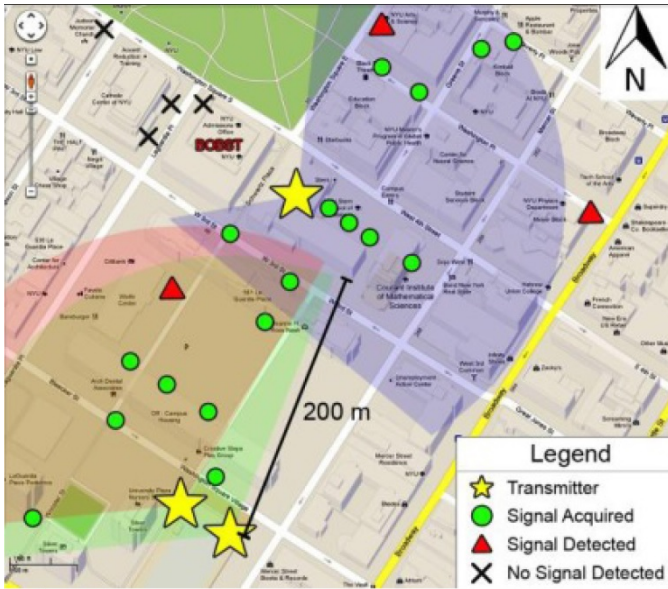


Fig. 1. Propagation Measurements

within the radius of 200m most of the location point to signal acquired with few pointing to signal detected and very less to outage, which concludes that 200m radius is a very reliable option in urban areas (as seen from figure also). It has been found that there is very high difference in propagation parameter in urban and semi-urban areas. Multipath fading is found to be very large in urban areas due to more reflections. Small scale fading which is fading experienced when a slight amount of change in location of receiver (in order of wavelength) does not change much when using highly directional antennas. Since signals could not propagate the outdoor building it is suggested to use access points/repeaters at the entrances of these building for smooth handover.

MIMO has a reputation of achieving a very high channel capacity for wireless systems. The major challenges that has appear in MIMO specially for mm-wave communication systems is about number of antennas, spacing between antenna. At mm wave frequencies the wavelength of the signal become very small hence the minimum required spacing between the antennas also reduces which result in high antennas carrying capacity on a single chip which can be steered for achieving adequate gain using optimum beamformer. As the antennas comes close ti space the signal beamformed are highly correlated which influence the transmitter and receiver correlation coefficient. These coefficients are used for modelling the channel as we do in Jakes model. High correlation among paths results in loss of information about the channel. Channel coefficients plays a pivotal role in calculating the capacity of the channels. Hence the above paragraph summarize some important challenges in the field of MM-wave wireless communication.

This paper is an extension of a SISO based time cluster-spatial lobe clustering algorithm for a mm-wave to MIMO channel model. The power delay profile for the mimo system is

generated using a spatial auto correlation function considering a small scale fading of multipath component for an arbitrary antenna pattern.

II. PATH LOSS AND CHANNEL MODEL

A. Large-scale and Scale-scale Fading

We will try to model path loss in conventional ways taking into consideration the constraints posed by mm-wave communication. Path loss (or path attenuation) is the reduction in power density (attenuation) of an electromagnetic wave as it propagates through space. Line of sight propagation is similar to free space communication where signal travels without any loss of power and NLOS components reaches the receiver with loss of power and delay according to path length and environment. These components when received at the receiver are super imposed. For eg. for a N path channel.

$$\tilde{h}(\tau) = \sum_{n=1}^N a_n \delta(\tau - \tau_n), \tau_n = l_n/c; \quad (1)$$

where a_n ad τ_n denotes the attenuation and the delay suffered by the n_{th} component of the signal received, c denotes the speed of light, l_n path length of n_{th} component. In this model we will consider that the flat faded channel i.e. $|a_n|$ and N are constant attributes of a static channel.

The major objective of the path loss model is to find the average power the lies in the local area for which we need to take the average of the power contained in the samples before doing the measurement for other parameter. Above point is supported by the fact that as the location of transmitter or receiver changes the delay and phases of signal phase changes (fast fading scenerio) but the average received power remains the same. The channel coefficients we will receiver will be the FIR version of the actual signal containing K bandlimited CIRs $h_k(\tau)$ The path loss can be written as

$$\tilde{h}(\tau) = -10 \log_{10} \frac{1}{K} \sum_{k=1}^K G_{C,k} \quad (2)$$

where $G_{C,k}$ is the channel gain received at k_{th} receiver denoted by

$$G_{C,k} = \int_0^{\tau_{max}} |h_k(\tau)|^2 d\tau \quad (3)$$

in above equation τ_{max} denotes the maximum delay the inner arguments in the (2) equation gives instantaneous power loss which will be equal to equation (3) if there is not fast fading and channel remains more or less constant.

B. Path Loss Model

The log-distance path loss model is a radio propagation model that predicts the path loss a signal encounters inside a building or densely populated areas over distance. In modeling the path loss we will take help from a well established exponent single slope long distance law which found its roots in frii's space and loss equation with $\bar{L}_{PL}(d_0)$, d , d_0 , X_σ are notation for reference or calibrated loss, actual distance,

reference distance and 0 mean, σ standard deviation Gaussian random variable.

$$L_{PL}(d)_{db} = \bar{L}_{PL}(d_0)_{db} + 10n \log_{10}\left(\frac{d}{d_0}\right) + X_\sigma \quad (4)$$

In this model we are able to find the loss of power with respect to one reference point which in multipath case can be considered as LOS component. This model helps in classifying the amount of loss each multipath component is suffering. If we are able to quantify it properly then we can choose significant components for FIR channel taps.

C. Channel Impulse Response

We have tried to model the high frequency radio channel in three dimensions using the concept of time clustering. Time clustering technique clubs all the signal components arriving in short span of time and groups them for classification which is done based upon their spread in the domain of angle. All these signals received together mostly suffer different delays and are received from different angles of azimuth and elevation and is solved as a classification problem. The spatial lobe in the name is majorly because of the reception of the signal from various directions of angle of arrival. The performance of the algorithm majorly depends upon the windowing time and intensity of the lobe scanning components. As we know the multipath components are received over a span of 100ns so it is important to classify them as first order and second order components allowing a partition window of 25ns. The model is parameterized using $a_k, \phi_k, \theta_k, \tau_k, \phi$ and θ which are nothing but attenuation for k th path, angle of arrival for k th path, azimuthal angle for k th path and delay for them and with last two giving the same for the LOS component.

$$h(t, \phi, \theta) = \sum_{k=1}^K a_k e^{j\phi_k} \delta(t - \tau_k) \cdot \delta(\phi - \phi_k) \cdot \delta(\theta - \theta_k) \quad (5)$$

The same model can be expressed in matrix form for H_l representing the stochastic evolution for l_{th} path where H_l denotes the $N_r \times N_t$ MIMO channel matrix of the l_{th} multipath component in an omnidirectional channel impulse response, expressed as in (2) [14]:

$$H_l = R_r^{1/2} \cdot H_w \cdot R_t^{1/2} \quad (6)$$

where R_r and R_t are the receive and transmit spatial correlation matrices. The matrix H_w is specified for the small scale fading path amplitudes. If the spatial components are considered to be uncorrelated then R_r and R_t will turn out to be identity matrices. The above representation is equivalent to SVD in the simple MIMO with pre and post matrix with row and column space to be orthogonal respectively.

These are some of the steps which the author has performed in order to find MIMO channel capacity and channel impulse response.

- 1 Generate one initial CIR using (1), from the mmWave SISO channel model in [10]. This is the mean spatially averaged CIR.

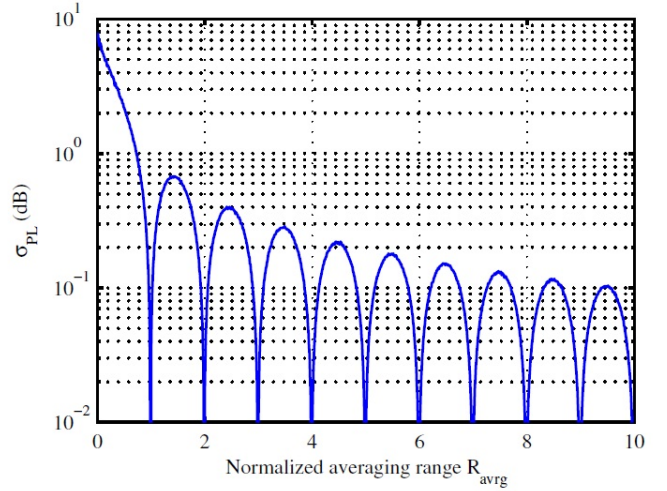


Fig. 2. Standard deviation of the estimated PL as a function of the normalized averaging range

- 2 For each generated multipath component in the initial CIR, generate $N_r \times N_t$ local "copies" over the local area, using (2), such that the voltage magnitudes obey the spatial correlation specified by R_r and R_t and the small-scale distribution specified by H_w . The multipath delays, AODs, and AOA of each multipath copy over the local area remain identical to the delays and angles in the initial CIR.
- 3 Compute the frequency response H_f of the MIMO channel impulse response H_l using a discrete Fourier transform operation.
- 4 Compute the total wideband capacity from (3) [6]:

$$G_{C,k} = \int_{f_{min}}^{f_{max}} \log_2 \det(I + \frac{\rho}{N_t} H_f H_f^H) df \quad (7)$$

where BW denotes bandwidth, ρ represents the average SNR, f_{min} and f_{max} denote the minimum and maximum narrowband sub-carrier frequencies, respectively.

III. AUTOCORRELATION, BANDWIDTH AND RESOLUTION

As we know that fast fading and frequency selective fading find their relation from the concept of average delay and coherence time. Flat fading can be achieved if the channel bandwidth is large enough and slow fading if coherence time is large. If we consider that n th path is suffering a delay of τ_n and a path length of l_n with $l_n = c \times \tau_n$. As we know that the relative time difference and inter-arrival times depend upon the nature of medium and location of scatterers.

$$B \geq [\min_{n=1, \dots, N-1} (\delta\tau_n)]^{-1} \quad (8)$$

The author has taken some important observations from the measurements he had. Unlike low frequency broadcast at mm wave there are very few number of paths which contribute (mainly like LOS and some other components). A very simple

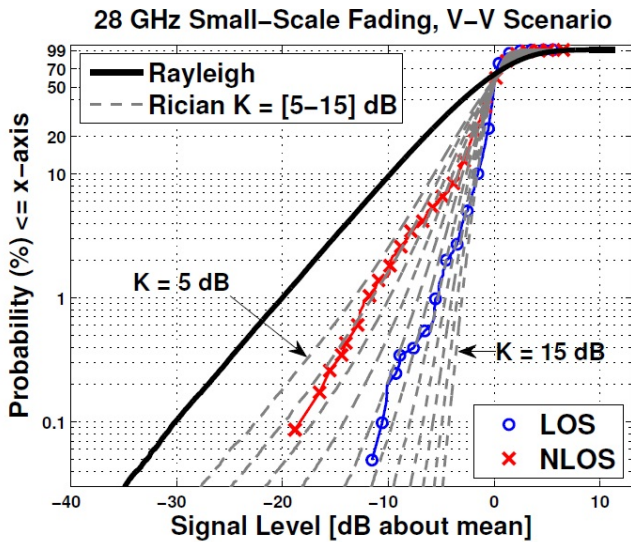


Fig. 3. Standard deviation and central fluctuation interval of σ_m as a function of the sample size for two different sampling ranges $[d_{min,m}, d_{max}]$

TABLE I

TABLE SUMMARIZING THE RANGES OF K-FACTORS FOR THE RICIAN DISTRIBUTIONS, DESCRIBING THE PATH (VOLTAGE) GAINS A_k IN (1), OBTAINED FROM 28 GHz DIRECTIONAL SMALL-SCALE FADING MEASUREMENTS OVER A LOCAL AREA IN DIFFERENT ENVIRONMENTS, FOR V-V AND V-H POLARIZATION CONFIGURATIONS.

Environment	$K_{VV}(dB)$	$K_{VH}(dB)$
LOS	9-15	3-7
NLOS	5-8	3-7
LOS-to-NLOS	4-7	6-10

such case is which a ground reflected wave interfere with the LOS famously known as **two ray phenomena**. In this case the path difference between two wave is:

$$\Delta l = \sqrt{d^2 + (h_t + h_r)^2} - \sqrt{d^2 + (h_t - h_r)^2} \quad (9)$$

$$\approx \frac{2h_t \cdot h_r}{d} \quad (10)$$

These equation can be extended to calculate the bandwidth for mm wave small scale fading channel which is given as:

$$BW = \frac{d_{max}c}{2h_t \cdot h_r} \quad (11)$$

It can be observed that even for a simple scenario with $h_t=3.5m$, $h_r=1.5m$ $d_{max}=100$ m the bandwidth required should be greater than 3 GHz.

A. MEASUREMENT and SIMULATIONS

Measurements are performed by author using the experimental setup at 28 GHz using 400 Mcps with gain of 15dB and setting some other parameters which arnot of that practical interest.

These measurements are performed in order to find the pdf which the fading channel possesses, autocorrelation function so as to calculate the channel taps for channel modeling. A

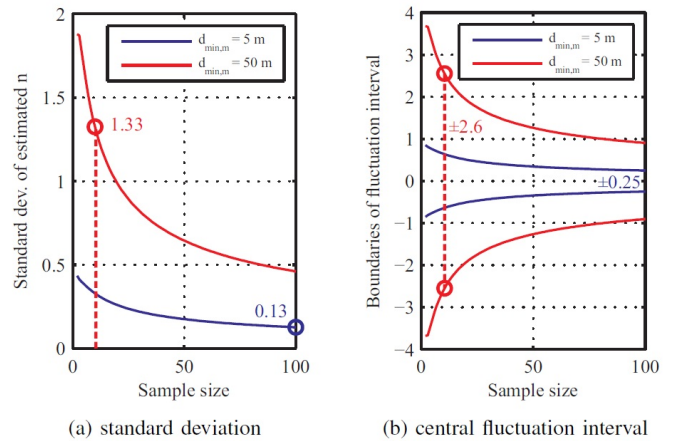


Fig. 4. CDF of 28 GHz measurement-based small-scale spatial fading distributions in LOS and NLOS scenarios.

number of observation were taken for known resul and it was noticed that the CDF for $\frac{|a_k|^2}{|a_k|}$ is following rician cumulative distribution unlike low frequency where they follow rayleigh fading. The other object was to find the autocorrelation function which was set up as :

$$f(\Delta r) = A \cdot e^{-B(\Delta r)} - C. \quad (12)$$

using curve fitting algorithm for the recorded observation the f was observed to be exponentially falling with $A=.99, B=1.95, C=0$; and for $A=.9$ the other two values were 1.5 and .1 respectively.

IV. SIMULATION RESULTS:

A. Limited Sample Size:

It is assumed that the PL actually follows (4). The sample size is limited to Formula PL values related to the distances Formula. The PL samples are ideal - in the sense that they are not subjected to small-scale fading or noise - and the parameters of the model (4) are estimated by linear regression in the LS sense. We exemplarily analyze the estimated PL exponent Formula. The theory related to linear regression and LS estimation tells us that Formula is normally distributed with the variance

$$Var \hat{\nu} = \frac{\sigma^2}{100} \left(\frac{1}{K} + \frac{\bar{x}^2}{(K-1)s_x^2} \right), \quad (13)$$

where

$$\bar{x} = \frac{1}{K} \sum_{k=1}^K x_k \text{ and } s_x^2 = \frac{1}{K-1} \sum_{k=1}^K (x_k - \bar{x})^2 \quad (14)$$

with

$$x_k = \log_{10} \left(\frac{a_k}{d_{ref}} \right) \quad (15)$$

It is obvious that Var Formula increases when Formula increases, but Formula is fixed for a given propagation scenario and cannot be influenced. Figure 4a shows the standard deviation σ_n (square root of (13)) of the estimation error as a

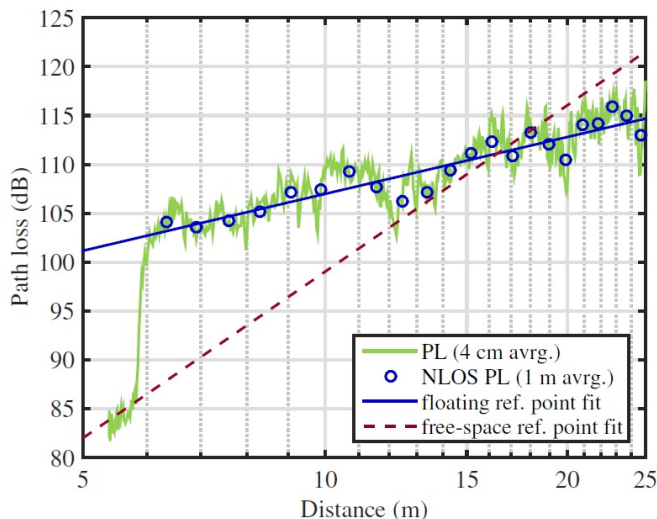


Fig. 5. Measured 60 GHz path loss for transition from LOS to NLOS..

function of the sample size \mathbf{K} for two different cases. In the first case, the samples are distributed over the whole range ($d_{min,m} = d_{ref} = 5m$), whereas the values are concentrated in the upper part in the second case ($d_{min,m} = 50m$). It is obvious that the distance range of the samples has a big impact: for $\mathbf{K} = 2$ (first value in Figure 4a), $\hat{\sigma}_n$ is more that four times as large for ($d_{min,m} = 50m$) compared to ($d_{min,m} = 5m$) (1.88 vs. 0.45). In order to achieve the same error as for $\mathbf{K} = 2$ and ($d_{min,meas} = 5m$), $\mathbf{K}_i 2$ would be required for $d_{min,m} = 50m$. If we denote $d_{min,m} = 5m$ in combination with $\mathbf{K} = 100$ as good Case 1 and $d_{min,m} = 50m$ with $\mathbf{K} = 10$ as bad Case 2, $\hat{\sigma}_n$ is approx. 10 times larger for Case 2 compared to Case 1 (1.33 vs. 0.13, see Figure 4a). The central fluctuation interval of \hat{n} with respect to a confidence level of 95% is shown in Figure 4b. The interval is proportional to $\hat{\sigma}_n$, and consequently, approx. 10 times larger for Case 2 Formula compared to Case 1 (± 0.25). It shall be stressed that a fluctuation interval of ± 2.6 means that, assuming e.g. $n=2$, the linear regression may yield values in the range $\hat{n} = -0.6|4.6$. Such large estimation errors, of course, are not acceptable.

B. Path Loss Model Reference Point :

In the current literature on mm-wave outdoor PL modeling, the intercept point in (4) is often set to the free-space value (free-space reference point, FSRP), instead of determining it by a free fit of measurement data (floating reference point, FRP). This is reasonable and helpful for LOS scenarios. Figure 5 shows a characteristic example of the measured path loss at 60 GHz as the RX moves behind a building. The propagation conditions change from LOS to NLOS between $d=5.8$ and 6.0 m. As expected, the PL increases abruptly, by approx. 17 dB in the shown example. For illustration it is assumed that the NLOS part of the data should be modeled by the FRP or the FSRP model. Figure 5 shows the corresponding LS fits to the averaged samples (1 m averaging) with $d_{ref} = 5m$. It is obvious that they largely differ. From the plots it can be

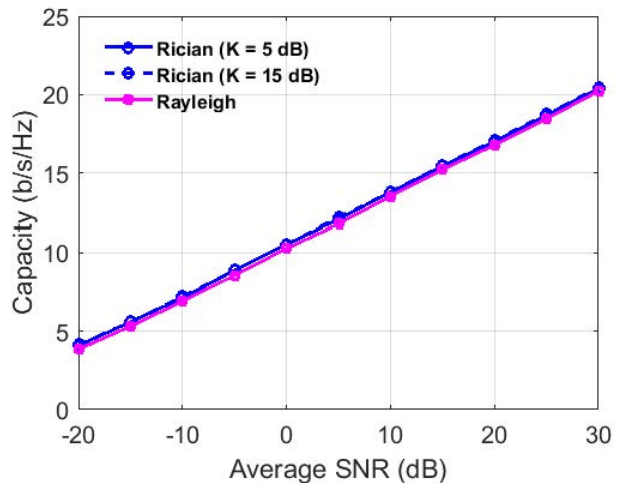


Fig. 6. Comparison of SIMO channel capacity between Rayleigh and Rician distributed small-scale fading coefficients with Rician K factors of 5 dB and 15 dB at 28 GHz. A single antenna is used at the transmitter, and a ULA with 20 elements is used at the receiver

summarized that

- 1) using the FSRP for NLOS data actually is a mixed LOS/NLOS modeling approach
- 2) the FSRP model is ill-suited for fitting pure NLOS data - it may significantly underestimate the PL at small distances.
- 3) NLOS PL exponents of the FRP and the FSRP model cannot be compared. It is hence highly recommended to use the FRP for NLOS modeling.

C. Median Path Loss :

In order to estimate the local path loss, we focused on mitigating small-scale effects by using the median value which has several advantages. The median is more robust against measurement errors and may considerably increase the accuracy of the estimation close to the noise floor.

Fig. 5 compares the SIMO channel capacity using Rayleigh and Rician distributed small-scale spatial fading coefficients with Rician K factors of 5 dB and 15 dB, using Eq. (3). The Rician distribution yields slight improvement (about 0.3 b/s/Hz) in capacity compared to the Rayleigh distribution. The physical interpretation is that the smaller the number of antennas, the fewer the number of spatial streams, thus a strong component will contribute significant channel capacity; when there are many antennas, we can exploit the MPCs to a large extent, hence the more MPCs the larger the capacity. Fig. 6 compares the MIMO channel capacity between Rayleigh and Rician small-scale distributions with Rician K factors of 5 dB and 15 dB at 28 GHz. It is observed that the Rayleigh distribution yields the highest capacity, while the lowest capacity is associated with the Rician distribution with a K factor of 15 dB, i.e., the lower the K factor, the higher the capacity in this case. Rician channels may result in greater or smaller capacity compared to Rayleigh channels, depending on the number of antennas due to the compromise between multipath exploitation and fading reduction.

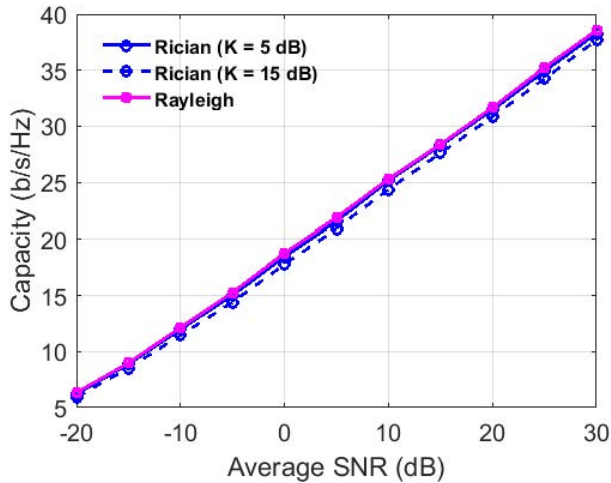


Fig. 7. CDF of 28 GHz measurement-based small-scale spatial fading distributions in LOS and NLOS scenarios.

REFERENCES

- [1] Mathew K. Samimi, Shu Sun, and Theodore S. Rappaport, *MIMO Channel Modeling and Capacity Analysis for 5G Millimeter-Wave Wireless Systems*
- [2] A. Paulraj et al., An overview of mimo communications - a key to gigabit wireless, *Proceedings of the IEEE*, vol. 92, no. 2, pp. 198218, Feb 2004.
- [3] T. S. Rappaport et al., *Millimeter Wave Wireless Communications*. Pearson/Prentice Hall 2015. Spatial Channel Model for Multiple Input Multiple Output (MIMO) Simulations, Tech. Rep. 3GPP 25.996 V12.0.0, Sept. 2014.
- [4] P. Kyosti et al., WINNER II channel models, European Commission, IST-WINNER, Tech. Rep. D1.1.2, Sept. 2007.
- [5] D. Shiu et al., Fading correlation and its effect on the capacity of multielement
- [6] antenna systems, *IEEE Transactions on Communications*, vol. 48, no. 3, pp. 502513, Mar. 2000.
- [7] J. Salo, L. Vuokko, H. El-Sallabi, and P. Vainikainen, Shadow fading revisited, in *Vehicular Technology Conference, 2006. VTC 2006-Spring*. IEEE 63rd, vol. 6, 2006, pp. 28432847.
- [8] T. Jms and T. S. Rappaport, Harmonization of 5G path loss models, in *COST IC1004 10th Management Committee and Scientific Meeting*, 2014.
- [9] H. Friis, A note on a simple transmission formula, *Proceedings of the IRE*, vol. 34, no. 5, pp. 254256, 1946.
- [10] T. Abbas, C. Gustafson, and F. Tufvesson, Pathloss estimation techniques for incomplete channel measurement data, in *COST IC1004 10th Management Committee and Scientific Meeting*, 2014.
- [11] W. Keusgen, R. J. Weiler, M. Peter, and M. Wisotzki, Propagation measurements and simulations for millimeter-wave mobile access in a busy urban environment, in *9th International Conference on Infrared, Millimeter, and Terahertz Waves, IRMMW-THz 2014*, Sep 1419, Tucson, USA, 2014.
- [12] R. J. Weiler, M. Peter, W. Keusgen, and M. Wisotzki, Measuring the busy urban 60 GHz outdoor access radio channel (invited), in *IEEE International Conferenc*